

ARM

CLIMATE RESEARCH FACILITY

Aerosol Observing System HANDBOOK



January 2011



U.S. DEPARTMENT OF
ENERGY

Office of
Science

DISCLAIMER

This report was prepared as an account of work sponsored by the U.S. Government. Neither the United States nor any agency thereof, nor any of their employees, makes any warranty, express or implied, or assumes any legal liability or responsibility for the accuracy, completeness, or usefulness of any information, apparatus, product, or process disclosed, or represents that its use would not infringe privately owned rights. Reference herein to any specific commercial product, process, or service by trade name, trademark, manufacturer, or otherwise, does not necessarily constitute or imply its endorsement, recommendation, or favoring by the U.S. Government or any agency thereof. The views and opinions of authors expressed herein do not necessarily state or reflect those of the U.S. Government or any agency thereof.

Aerosol Observing System (AOS) Handbook

A. Jefferson

January 2011

Work supported by the U.S. Department of Energy,
Office of Science, Office of Biological and Environmental Research

Contents

1.0	General Overview of AOS	1
2.0	Timeline and Deployment History	1
3.0	Data Description	2
3.1	File Variables and Format	2
3.2	Data Quality Flags	3
3.3	Diagnostic Variables	4
3.4	Data Uncertainty	4
4.0	Data Examples	6
5.0	Value-Added Products	8
5.1	Aerosol Intensive Properties	8
5.2	Aerosol Scattering Hygroscopic Growth, fRH	9
5.3	Aerosol Best Estimate	9
5.4	CCN Power Law Fit Parameter	9
6.0	Data Quality and Status	9
6.1	Data Quality Health and Status	9
6.2	Mentor Reports	9
7.0	Instruments and Measurement Details	10
7.1	List of Instruments	10
7.2	System Configuration and Measurements Methods	10
7.3	Calibrations	11
7.4	Operations and Maintenance	12
8.0	Retired Measurements	13
8.1	Ozone Monitor	13
8.2	Optical Particle Counter	13
8.3	Aerosol Inorganic Ion Composition	13
9.0	References	14
	Appendix A – Aerosol Hygroscopic Growth Measurements	A.1
	Appendix B – Cloud Condensation Nuclei Measurements	B.1

Figures

1	Aerosol absorption coefficient at 550 nm for both submicron and sub-10-micron particle sizes.....	6
2	Aerosol scattering coefficient at 550 nm for both submicron and sub-10-micron particle sizes.....	7
3	Aerosol single scatter albedo at SGP for submicron and sub-10-micron size aerosol from November 23–29, 2010.....	7
4	Aerosol scattering Ångstrom exponent at SGP for submicron and sub-10-micron size aerosol from November 23–29, 2010.....	8
5	AOS flow schematic.....	11

Tables

1	Measured aerosol properties from the AOS.....	2
2	AOS flag fields	3
3	Diagnostic variables in the AOS datastream.....	4
4	Instrument noise, drift, and uncertainty factors.....	5

1.0 General Overview of AOS

The Aerosol Observing System (AOS) is a suite of in situ surface measurements of aerosol optical and cloud-forming properties. The instruments measure aerosol properties that influence the earth's radiative balance. The primary optical measurements are those of the aerosol scattering and absorption coefficients as a function of particle size and radiation wavelength and cloud condensation nuclei (CCN) measurements as a function of percent supersaturation. Additional measurements include those of the particle number concentration and scattering hygroscopic growth. Aerosol optical measurements are useful for calculating parameters used in radiative forcing calculations such as the aerosol single-scattering albedo, asymmetry parameter, mass scattering efficiency, and hygroscopic growth. CCN measurements are important in cloud microphysical models to predict droplet formation.

The system is located at the Southern Great Plains (SGP) site in Oklahoma and has been operational since the beginning of April 1996. From 1997–2010, the Aerosol Group at the National Oceanic and Atmospheric Administration's (NOAA)/Earth System Research Laboratory (ESRL)/Global Monitoring Division (GMD) had mentorship of the AOS. In March of 2005 a second AOS system was installed as part of the ARM Mobile Facility (AMF). ARM also archives AOS data from the NOAA Barrow Observatory in Barrow, Alaska at the North Slope of Alaska (NSA). Since 2011 the mentorship is a collaborative arrangement between the NOAA/ESRL/GMD group and the Cooperative Institute for Research in the Environmental Science (CIRES) at the University of Colorado.

2.0 Timeline and Deployment History

SGP: April 1996–present

NSA: (NOAA BRW Observatory) 1998–present

AMF:

- PYE: March–September 2005; Pt. Reyes, California, USA
- NIM: December 2005–December 2006; Niamey, Niger
- FKB: April 2007–December 2007; Heselbach, Germany
- HFE: June 2008 –December 2008; Shouxian, China
- GRW: May 2009–December 2010; Graciosa Island, the Azores, Portugal
- PGH: April 2011–March 2012; Nainital, India

Future AMF deployments and site descriptions are at <http://www.arm.gov/sites/amf>.

3.0 Data Description

3.1 File Variables and Format

The current netcdf file description is located at

<https://engineering.arm.gov/tool/dod/showdod.php?Inst=aos&View=user>

Table 1 describes the directly measured variables from the AOS system in the stnaosC1.a1 netcdf file.

Table 1. Measured aerosol properties from the AOS.

Variable Name	Quantity Measured	Unit
N_CPC	Condensation nuclei number concentration	1/cm ³
N_CCN	Cloud condensation nuclei number concentration	1/cm ³
Ba_G_Dry_10um	Aerosol absorption coefficient 550 nm, 10 um	1/m
Ba_G_Dry_1um	Aerosol absorption coefficient 550 nm, 1 um	1/m
Bs_B_Dry_10um	Aerosol scattering coefficient 450 nm, 10 um	1/m
Bs_B_Dry_1um	Aerosol scattering coefficient 450 nm, 1 um	1/m
Bs_G_Dry_10um	Aerosol scattering coefficient 550 nm, 10 um	1/m
Bs_G_Dry_1um	Aerosol scattering coefficient 550 nm, 1 um	1/m
Bs_R_Dry_10um	Aerosol scattering coefficient 700 nm, 10 um	1/m
Bs_R_Dry_1um	Aerosol scattering coefficient 700 nm, 1 um	1/m
Bbs_B_Dry_10um	Aerosol backscattering coefficient 450 nm, 10 um	1/m
Bbs_B_Dry_1um	Aerosol backscattering coefficient 450 nm, 1 um	1/m
Bbs_G_Dry_10um	Aerosol backscattering coefficient 550 nm, 10 um	1/m
Bbs_G_Dry_1um	Aerosol backscattering coefficient 550 nm, 1 um	1/m
Bbs_R_Dry_10um	Aerosol backscattering coefficient 700 nm, 10 um	1/m
Bbs_R_Dry_1um	Aerosol backscattering coefficient 700 nm, 1 um	1/m
Bs_B_Wet_10um	Aerosol humidified scattering coefficient 450 nm, 10 um	1/m
Bs_B_Wet_1um	Aerosol humidified scattering coefficient 450 nm, 1 um	1/m
Bs_G_Wet_10um	Aerosol humidified scattering coefficient 550 nm, 10 um	1/m
Bs_G_Wet_1um	Aerosol humidified scattering coefficient 550 nm, 1 um	1/m
Bs_R_Wet_10um	Aerosol humidified scattering coefficient 700 nm, 10 um	1/m
Bs_R_Wet_1um	Aerosol humidified scattering coefficient 700 nm, 1 um	1/m
Bbs_B_Wet_10um	Aerosol humidified backscattering coefficient 450nm, 10um	1/m
Bbs_B_Wet_1um	Aerosol humidified backscattering coefficient 450 nm, 1um	1/m
Bbs_G_Wet_10um	Aerosol humidified backscattering coefficient 550 nm, 10um	1/m
Bbs_G_Wet_1um	Aerosol humidified backscattering coefficient 550 nm, 1um	1/m
Bbs_R_Wet_10um	Aerosol humidified backscattering coefficient 700 nm, 10um	1/m
Bbs_R_Wet_1um	Aerosol humidified backscattering coefficient 700 nm, 1um	1/m
Ba_B_Dry_10um_PSAP3W	Aerosol absorption coefficient 467 nm, 10 um	1/m
Ba_B_Dry_10um_PSAP3W	Aerosol absorption coefficient 467 nm, 1 um	1/m
Ba_B_Dry_10um_PSAP3W	Aerosol absorption coefficient 530 nm, 10 um	1/m
Ba_B_Dry_10um_PSAP3W	Aerosol absorption coefficient 530 nm, 1 um	1/m
Ba_B_Dry_10um_PSAP3W	Aerosol absorption coefficient 660 nm, 10 um	1/m
Ba_B_Dry_10um_PSAP3W	Aerosol absorption coefficient 660 nm, 1 um	1/m

3.2 Data Quality Flags

A data flag designates the sampling conditions and level of data processing. The flag field is in hexadecimal format. Of particular importance is the third character bit, which designates the aerosol impactor sampling size. The aerosol sampling switches every 30 minutes between sub-10-micron (0000) and submicron (0010) size aerosol. Table 2 lists the flags and their designations.

Table 2. AOS flag fields

Bit Position	Hex Bit Mask	Description	Bit Set (1)	Bit Clear (0)
1				
1:3	8000	Not used		
1:2	4000	Not used		
1:1	2000	Not used		
1:0	1000	Not used		
2		Data Corrections		
2:3	0800	Dilution	Applied	Not applied
2:2	0400	Neph truncation	Applied	Not applied
2:1	0200	Psap spot and flow corrections	Applied	Not applied
2:0	0100	STP	Applied	Not applied
3		Sampling Conditions		
3:3	0080	Not used		
3:2	0040	Not used		
3:1	0020	Psap transmission (Tr)	Tr <0.7	Tr >0.7
3:0	0010	Impactor size	submicron	Sub 10 micron
4		Sampling Conditions		
4:3	0008	Not used		
4:2	0004	Wind Sector	Pollution	Clean
4:1	0002	Manual contamination control	Pollution	Clean
4:0	0001	Automatic contamination control	Pollution	Clean

3.3 Diagnostic Variables

The diagnostic variables in the AOS datastream include those of the instrument temperature, pressure, RH, wind speed, and direction. A description of each parameter is given in Table 3. The ambient variables as well as wind speed and direction are not merged in all of the AOS datastreams.

Table 3. Diagnostic variables in the AOS datastream.

Variable name	Description	Unit
RH_MainInlet	RH at impactor inlet	%
T_MainInlet	Temperature at impactor inlet	°C
RH_NephInlet_Dry	RH at dry nephelometer inlet	%
T_NephInlet_Dry	Temperature at dry nephelometer inlet	°C
RH_NephVol_Dry	RH inside the dry nephelometer	%
T_NephVol_Dry	Temperature inside the dry nephelometer	°C
RH_preHG	RH before the humidifier	%
T_preHG	Temperature before the humidifier	°C
RH_postHG	RH after the humidifier	%
T_postHG	Temperature after the humidifier	°C
RH_NephInlet_Wet	RH at inlet of wet nephelometer	%
T_NephInlet_Wet	Temperature at inlet of wet nephelometer	°C
RH_NephVol_Wet	RH inside wet nephelometer	%
T_NephVol_Wet	Temperature inside wet nephelometer	°C
RH_ambient	Ambient RH	%
T_ambient	Ambient temperature	°C
P_ambient	Ambient pressure	hPa
P_Neph_Dry	Pressure inside dry nephelometer	hPa
P_Neph_Wet	Pressure inside wet nephelometer	hPa
WindSpeed	Wind Speed	m/s
WindDirection	Wind Direction	degrees
Lat	Latitude	degrees
Lon	Longitude	Degrees
Alt	Altitude	m

3.4 Data Uncertainty

The calculation of the measurement uncertainty of each nephelometer follows the protocol of Anderson et al. (1999). The measurement uncertainty associated with the TSI 3563 nephelometer was calculated from five known sources and is expressed as a linear combination of the following terms:

$$du_{\text{total}}^2 = du_{\text{noise}}^2 + du_{\text{drift}}^2 + du_{\text{cal}}^2 + du_{\text{trunc}}^2 + du_{\text{stp}}^2.$$

Here, dup designates the uncertainty in u associated with the parameter, p . These arise from the following:

- instrument noise in the filtered air scattering coefficient
- instrument drift in the calibration
- uncertainty in the instrument calibration to Rayleigh scattering of dry air and CO_2
- instrument truncation of near forward scattered light
- uncertainty in the instrument pressure and temperature in conversion of the data to STP.

The associated uncertainties for each parameter for one-minute averages are listed in Table 4 as a function of the scattering coefficient magnitude.

Table 4. Instrument noise, drift, and uncertainty factors.

Bsp	Noise	Drift	Calibration	Truncation	STP	Total
1	1.25	0.44	0.08	0.02	0.003	1.33
10	1.56	0.80	0.75	0.22	0.03	1.92
20	1.84	1.20	1.50	0.44	0.07	1.70
50	2.50	2.40	3.75	1.10	0.17	5.23
100	3.32	4.40	7.51	2.10	0.34	9.58

Uncertainty associated with differences in the aerosol inlets and tubing is expected to be insignificant for submicron aerosol. Losses within the nephelometer itself were found to be negligible for submicron particles and are 5%–10% for super micrometer particles (Anderson and Ogren 1998). The variation in particle size with relative humidity (RH) and hence, the particle transmission through a submicron impactor, operating upstream of the nephelometer, will vary with the particle type. For an RH below 50%, we estimate this uncertainty to be less than 5% based on Berner impactor efficiency curves and estimates of the scattering size distribution. In addition to RH, the flow rate affects the 50% aerodynamic cutoff diameter of the impactor. Running the Berner-type impactors at a flow 10% lower than 30 lpm yields a 5% change in cut size. Typically, flows are within 1%–2% of the expected flow rate.

For low-scattering values, instrument noise is the prevalent source of uncertainty, while for higher scattering coefficients both noise and instrument truncation uncertainties dominate. Uncertainty for low signal values can be greatly reduced by increasing the signal averaging time. For a 10-min averaging time, the uncertainty associated with noise for a bsp of 1 Mm^{-1} is 0.40 Mm^{-1} . Truncation corrections for sub-10 μm and super- μm size particles are significantly higher than those for sub- μm size particles. See Anderson and Ogren 1998 and Heintzenburg et al. 2006 for discussions on the uncertainty of nephelometer scattering coefficients.

Uncertainty in the particle soot absorption photometer (PSAP) has been described by Sheridan et al. (2005) and Virkkula et al. (2010). Corrections have been made for spot size, flow rate, wavelength, interpretation of scattering as absorption, and instrument response to absorption (Bond et al. 2001 and Ogren 2010). Uncertainty in the measurements also stems from the variability of each PSAP unit and from instrument noise. Bond et al. found instrumental variability to be 6% of the measured absorption. Instrument noise (i.e. detection limit), determined by measuring particle-free air, is 0.1 Mm^{-1} for hourly

averaged data and 0.9 Mm^{-1} for minute-averaged data. The total uncertainty in aerosol absorption coefficient from the PSAP usually varies from 1 to 4 Mm^{-1} for one-minute average data and depends on the magnitudes of the absorption and scattering coefficients. PSAP noise and uncertainty was found to increase in high RH environments and in air with high concentrations of semi-volatile organics (Lack et al. 2008).

4.0 Data Examples

The data in Figures 1 and 2 show typical aerosol absorption and scattering coefficients at 550 nm for both aerosol size cuts. The data are from November 23–29, 2010 at SGP with one-minute integration times. The two colors indicate the two aerosol sizes, which change every 30 minutes. On day 328, November 24, larger supermicron aerosol are present, and the scattering between the two size cuts diverge. Because most of the absorbing aerosol resides in the submicron size range, there is little difference between the submicron and sub-10-micron absorption coefficients on this day. Figures 3 and 4 show the changes in the aerosol size and absorption properties during the same time period.

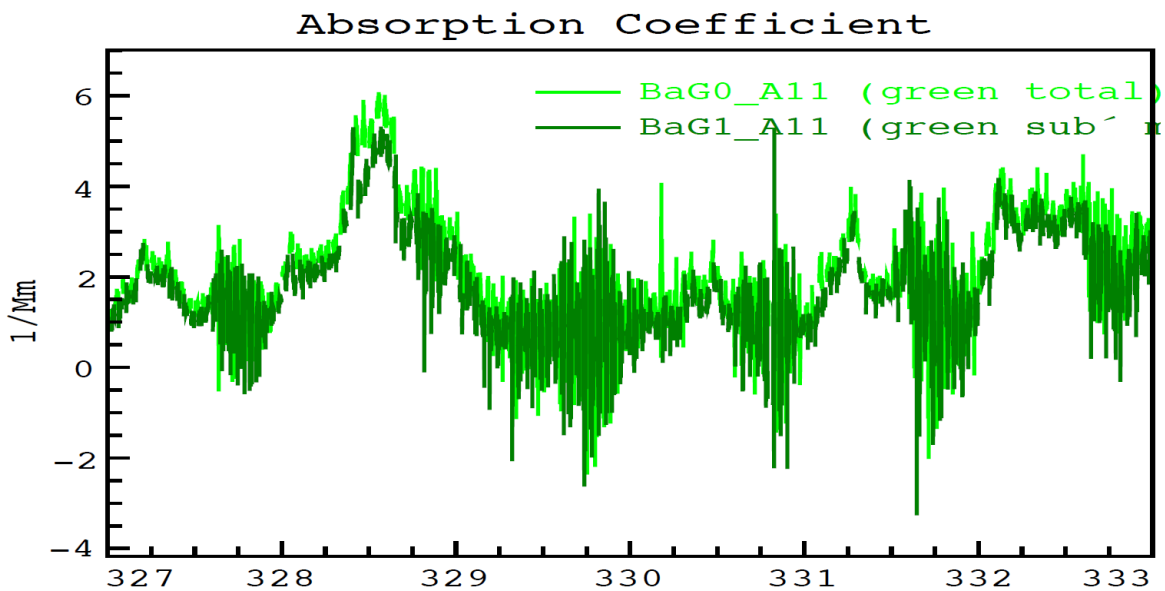


Figure 1. Aerosol absorption coefficient at 550 nm for both submicron and sub-10-micron particle sizes.

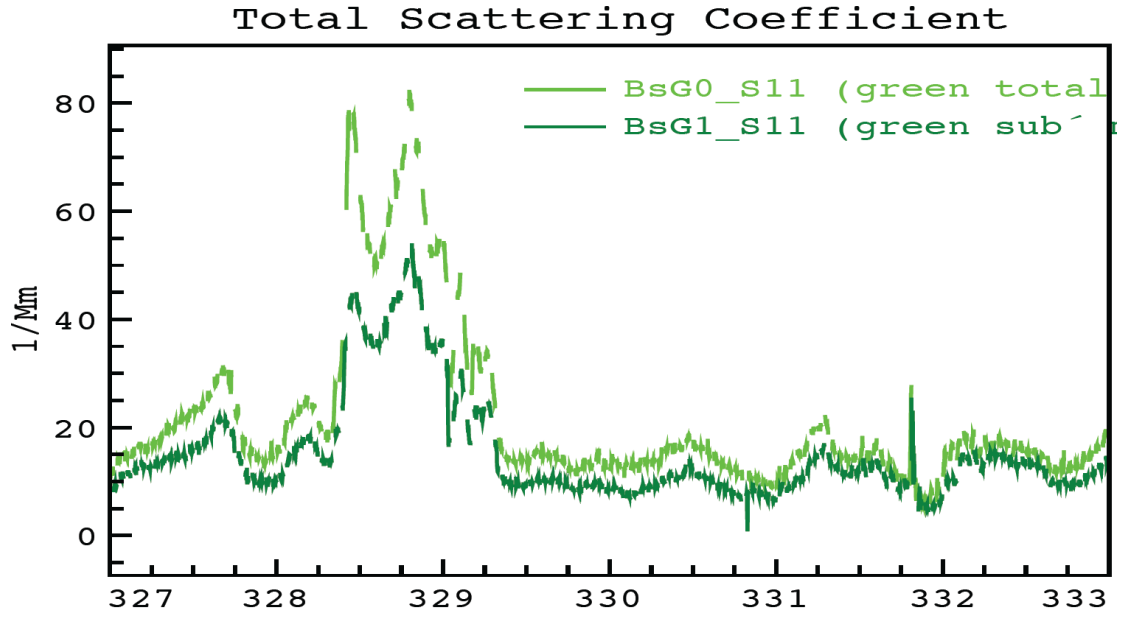


Figure 2. Aerosol scattering coefficient at 550 nm for both submicron and sub-10-micron particle sizes.

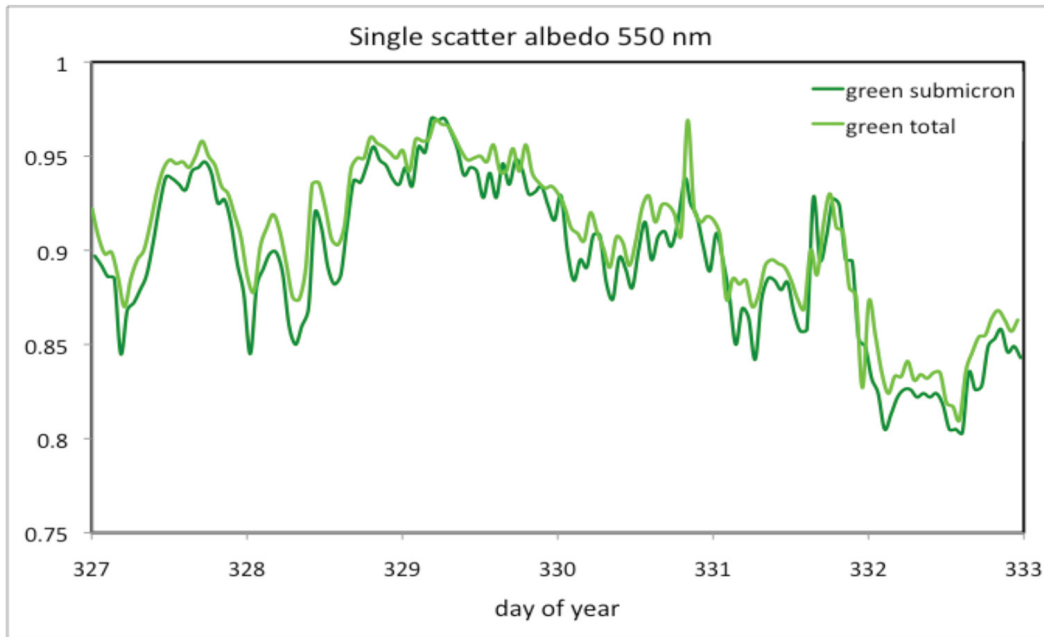


Figure 3. Aerosol single scatter albedo at SGP for submicron and sub-10-micron size aerosol from November 23–29, 2010.

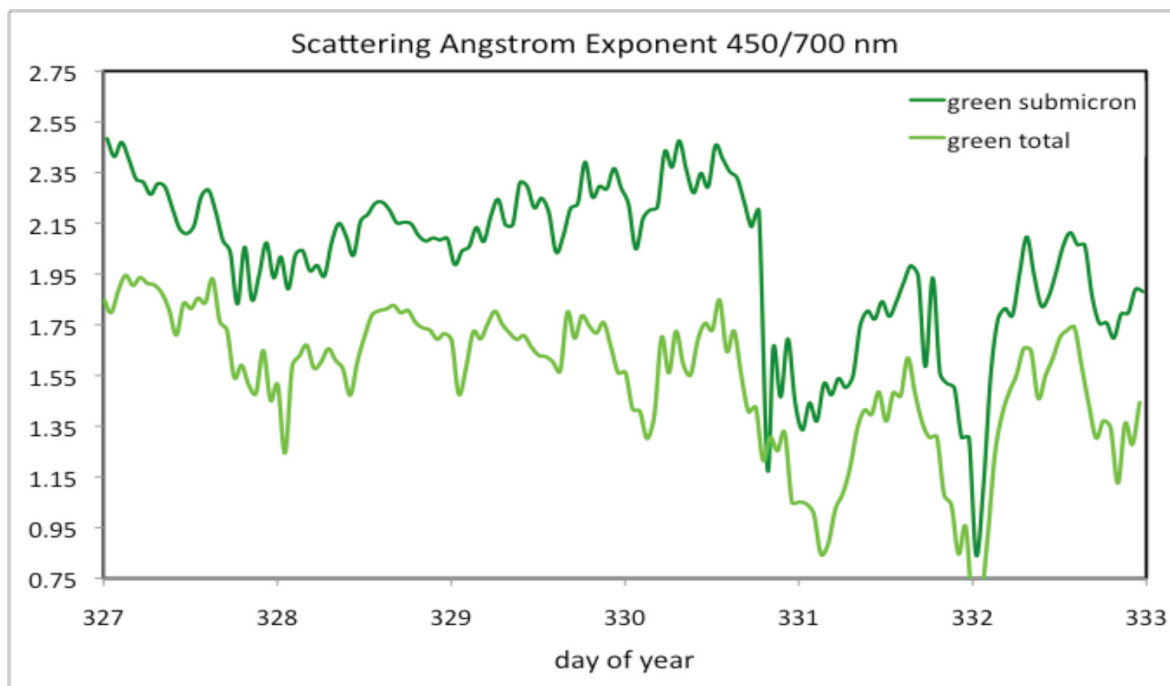


Figure 4. Aerosol scattering Ångstrom exponent at SGP for submicron and sub-10-micron size aerosol from November 23–29, 2010.

Figures 3 and 4 display the aerosol scattering albedo and Ångstrom exponents over the same time period as the data in Figures 1 and 2. The data in the figures are 30-minute averages. The relatively large separation in the Ångstrom exponents between the two size cuts suggests a significant fraction of coarse-mode aerosol was present. Differences between the aerosol scattering albedo in the two size cuts are small, with the total sub-10-micron aerosol having a slightly higher albedo than the submicron aerosol.

5.0 Value-Added Products (VAPs)

5.1 Aerosol Intensive Properties

The aerosol intensive properties are calculated properties from the measured extensive parameters. The intensive parameters calculated from the aerosol absorption, scattering, and backscattering coefficients are the single scatter albedo, hemispheric backscatter fraction, upscatter fraction, asymmetry parameter, submicron absorption fraction, submicron scattering fraction, aerosol forcing efficiency, and the absorption and scattering Ångstrom exponents. The intensive properties are located in two files: `sssaipogrenFn.c1` and `ssaaipavglogrenFn.c1`. The `sss` prefix designates the site location and `Fn` the facility at the site. The `aiplogren` files are one-minute averaged data, and the `aipavglogren` files are hourly averaged data. An extensive description of the file format, variable description, and calculation process is located on the ARM website at <http://science.arm.gov/vaps/aiplogren.stm>.

5.2 Aerosol Scattering Hygroscopic Growth, fRH

The aerosol hygroscopic growth is a measure of the increase in the aerosol scattering coefficient with relative humidity. A description of the humidified measurements and hygroscopic growth calculations is located in Appendix A. As of 2011 the hygroscopic growth VAP was still in its evaluation period and had not been released. Please contact the mentor for information on this VAP.

5.3 Aerosol Best Estimate

The Aerosol Best Estimate (ABE) product gives profiles of the aerosol intensive properties as a function of altitude. AOS and aipogren VAP data contribute to the ABE product. As of 2011 this product was still in its evaluation period.

5.4 CCN Power Law Fit Parameter

This product has yet to be evaluated. More information on it is available in Appendix B, which describes the CCN measurements and data.

6.0 Data Quality and Status

6.1 Data Quality Health and Status

An interactive plotting tool is available on the ARM Data Management Facility website, where users can plot recent or past AOS data from the various sites. The data-plotting tool is available at <http://plot.dmf.arm.gov/ncvweb/ncvweb.cgi>. The tool plots raw data from the most recent quarter. Recent and statistical plots of the AOS data are also available on the NOAA/ESRL/GMD website at <http://www.esrl.noaa.gov/gmd/aero/net/index.html>.

6.2 Mentor Reports

Data quality reports (DQRs) and Instrument Mentor Monthly Summaries (IMMS) are available from the ARM database at <http://www.db.arm.gov/>. The IMMS reports provide a monthly summary of both the data and the instrument operation. The DQRs identify problems with the data. Both report types should be checked prior to using AOS data.

7.0 Instruments and Measurement Details

7.1 List of Instruments

Aerosol instrumentation inside the trailer consists of the following:

1. Two nephelometers. These are 3-wavelength (450, 550, and 700 nm) TSI (Model 3563) nephelometers that measure total angular scattering and hemispheric backscattering coefficients from 90° to 170°. The second TSI nephelometer is connected to a humidity scanning system to provide 12 measurements of the scattering coefficients as a function of RH. A check of the nephelometer calibration with CO₂ gas is performed weekly.
2. Light absorption photometer. The Radiance Research (Model PSAP) Particle Soot Absorption Photometer measures the particle absorption coefficient at the wavelength of 550 nm. In April 2005, this instrument was upgraded to a 3-wavelength instrument (470, 528, and 660 nm).
3. Condensation nuclei counter. The TSI (Model 3010) measures the total number concentration of condensation particles of diameter in the size range of 10 nm to 3 μm.
4. Cloud Condensation Nuclei Counter (CCN), single-column DMT Model 1. The CCN measures the cloud droplet concentration at 7 supersaturations as well as the droplet size distribution from 1 μm to 10 μm in 20 size bins.
5. Continuous Light Absorption Photometer (CLAP), NOAA. The CLAP is a filter-based technique that measures the aerosol light absorption coefficient at three visible wavelengths, 470, 528, and 660 nm.

7.2 System Configuration and Measurements Methods

Figure 5 below shows the AOS flow schematic. About 800 lpm flow through an 8" diameter external stack. The sample air flows through a 2" diameter stainless steel pipe in the center of this larger flow. 120 lpm flows through the sample tube, which splits into five 30-lpm sample lines. At the AMF one of these sample lines goes into the AOS system, and the other 4 spare sample lines go out through a blower. At SGP the spare sample lines go to the HTDMA, ACSM, and PAAS instruments, and one line is used to monitor the temperature and RH at the exit of the sample flow splitter.

The nephelometer and PSAP instruments are downstream of a set of switched impactors. These impactors toggle the aerosol size cut between 1.0 μm and 10 μm aerodynamic particle diameters every 30 minutes. The advantage of measuring two aerosol size ranges is that fine and coarse mode aerosols often have different sources, and this method allows optical measurements of both aerosol types.

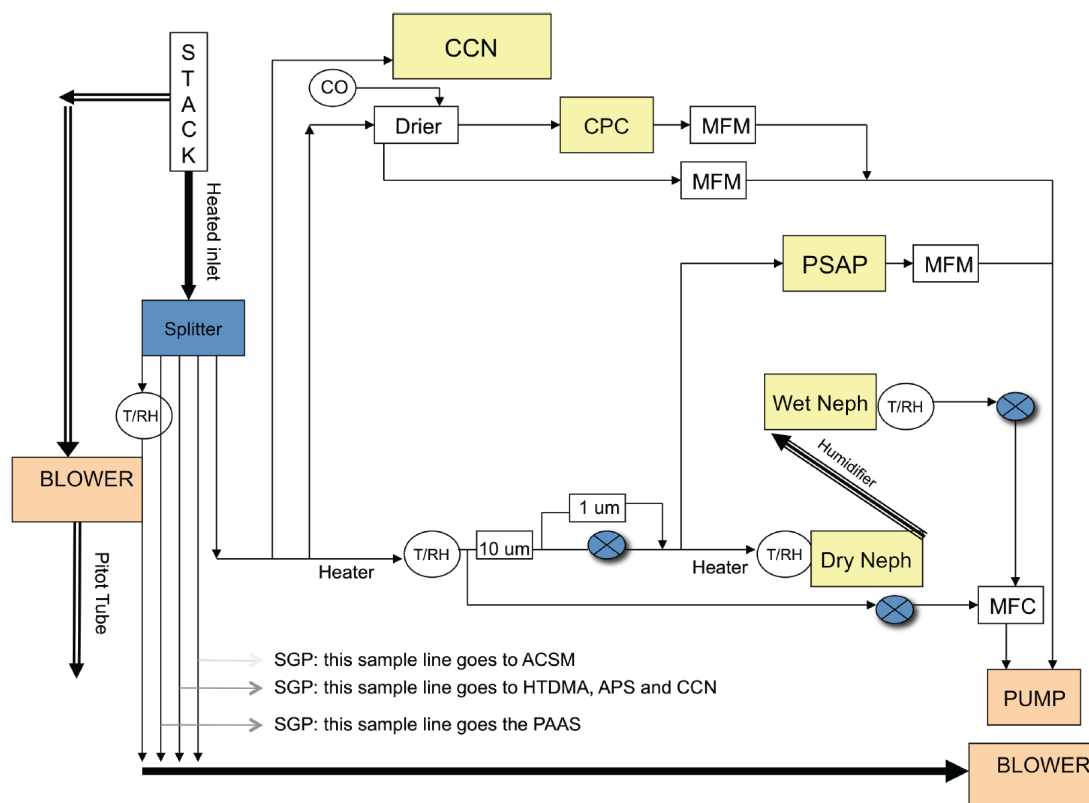


Figure 5. AOS flow schematic. Symbols represent the following: T/RH: temperature and relative humidity sensor; CO: critical orifice; MFM: mass flow meter; and MFC: mass flow controller. Blue Xs are valves.

The relative humidities of the four T/RH sensors shown in Figure 5 are regulated via PID (proportional, differential, and integrative) controllers. These PID controllers regulate the relative humidity at the output of the sample splitter and immediately upstream of the impactors to 40% RH. An RH of 40% was chosen to measure the properties of the intrinsic “dry” aerosol with minimal contribution from water and also to minimize evaporation of semi-volatile organics and acids from the aerosol. The RH immediately upstream of the reference or dry nephelometer and humidifier is controlled to 40%, and the RH after the wet nephelometer and humidifier is ramped hourly between about 40 to 85% RH. See Appendix A for information about the humidifier operation.

7.3 Calibrations

The instrument flow, pressure, temperature, and relative humidity sensors are calibrated annually. A Bios-brand flow standard is used to calibrate the instrument flows. The SGP facility maintains a Thunder Scientific RH and temperature calibration chamber that is traceable to NIST standards. The SGP and AMF Vaisala T/RH probes are calibrated in this chamber. A magnehelic gauge is used to calibrate the pressure sensors.

7.4 Operations and Maintenance

Daily Maintenance

- Check flows and vacuum readings
- Check instrument and computer communications
- Change PSAP and CLAP filter as needed
- Fill humidifier and CCN water supplies
- Fill CPC butanol as needed.

Weekly Maintenance

- CO² span check of nephelometers
- Clean impactors
- Change PSAP reference filter.

Periodic Maintenance

- Leak check of system
- Change neph lamp
- Clean CPC
- Drain and refill butanol in CPC.

Annual Maintenance

- Perform flow calibrations on main sample flow, cpc critical orifice , PSAP, and CCN sheath and sample flows
- Calibrate CCN pressure, impactor delta P, and blower pitot
- Clean CPC
- Replace CCN, mass flow meter, and neph hepa filters
- Clean CCN opc
- Bleach solution purge of CCN column
- Clean capillary sample tube in CCN
- Replace CCN pump diaphragm
- Leak check of CCN
- Remove files from CCN hard drive
- Clean inlet lines
- System leak check

- Update software
- Clean nephelometers
- Calibrate nephelometers
- Replace carbon vanes in pump
- Replace cracked or dirty tubing
- Clean or replace humidifier
- Replace nafion tubes before CPC and PSAP and in CCN
- Train site technician
- Perform inventory of AOS parts and spares.

8.0 Retired Measurements

8.1 Ozone Monitor

The Dasibi (Model 1008) ozone monitor measures the ozone mixing ratio between 1 and 1000 ppbv using monochromatic ultraviolet (UV) absorption spectrophotometry. This instrument was in operation at SGP from 1998–2004.

8.2 Optical Particle Counter

The PMS (Model PCASP-X) OPC measures the particle number concentration in 31 size channels from 0.1 to 10 μm . This instrument was inoperable and removed in 2004 because of poor instrument reliability. The data collection for this instrument spanned from 1997–2004. In 2008 a TSI model 3321 Aerodynamic Particle Sizer (APS) was installed as a complement to the HTDMA. The size range of the APS is 0.5 to 20 μm .

8.3 Aerosol Inorganic Ion Composition

Daily filter samples of aerosol were collected at SGP from 2000–2008. Patricia Quinn of NOAA PMEL analyzed the daily samples for the aerosol inorganic ion composition. Similar filter samples are collected at the NSA Barrow site that date from 1998 to the present. The sample duration at NSA varies from daily in the spring when aerosol loading is relatively high to one sample per week in the summer and fall when aerosol loading is low. Data from these filter samples are located on the PMEL web site at <http://saga.pmel.noaa.gov/>.

9.0 References

- Anderson, TL, and JA Ogren. 1998. "Determining aerosol radiative properties using the TSI 3563 integrating nephelometer." *Aerosol Science and Technology* 29: 57–69.
- Anderson, TL, DS Covert, JD Wheeler, JM Harris, KD Perry, BE Trost, DJ Jaffe, and JA Ogren. 1999. "Aerosol backscatter fraction and singlescattering albedo: Measured values and uncertainties at a coastal station in the Pacific Northwest." *Journal of Geophysical Research* 104: 26793–26807.
- Bond, TC, TL Anderson, and D Campbell. 2001. "Calibration and intercomparison of filter-based measurements of visible light absorption by aerosols." *Aerosol Science and Technology* 30: 582–600.
- Heintzenberg, J, A Wiedensohler, TM Tuch, DS Covert, P Sheridan, JA Ogren, J Gras, R Nessler, C Kleefeld, N Kalivitis, V Aaltonen, R-T Wilhelm, and M Havlicek. 2006. "Intercomparisons and aerosol calibrations of 12 commercial integrating nephelometers of three manufacturers." *Journal of Atmospheric and Oceanic Technology* 23(7): 902–914.
- Lack, DA, CD Cappa, DS Covert, T Baynard, P Massoli, B Sieru, TS Bates, PK Quinn, ER Lovejoy, and AR Ravishankara. 2008. "Bias in filter-based light absorption measurements due to organic aerosol loading: evidence from ambient measurements." *Aerosol Science and Technology* 42:1033–1041.
- Sheridan, PJ, DJ Delene, and JA Ogren. 2001. "Four years of continuous surface aerosol measurements from the Department of Energy's Atmospheric Radiation Measurement Program Southern Great Plains Cloud and Radiation Testbed site." *Journal of Geophysical Research* 106(D18): doi:10.1029/2001JD000785.
- Virkkula, A, NC Ahlquist, DS Covert, WP Arnott, PJ Sheridan, PK Quinn, and DJ Coffman. 2005. "Modification, calibration and a field test of an instrument for measuring light absorption by particles." *Aerosol Science and Technology* 39: 68–83.

Appendix A

Aerosol Hygroscopic Growth (*fRH*) Measurements

The AOS humidified nephelometer measures the increase in the aerosol scattering coefficient with relative humidity (RH). Figure A.1 shows a diagram of the humidifier setup. The instrument setup consists of two nephelometers in series with a humidifier between them. The “reference” nephelometer measures the dry aerosol scattering coefficients. The sample air moves through a humidifier, which steps the RH from about 40–85%, and the second nephelometer measures the aerosol scattering at the elevated RH. Actual RH values vary with the ambient dew point, sample residence time in the humidifier, water temperature, and humidifier porosity.

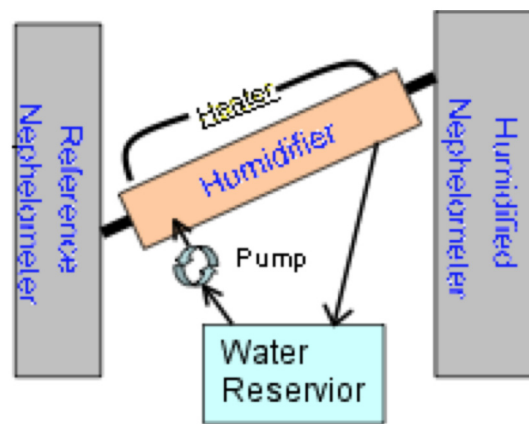


Figure A.1. Simplified diagram of humidified nephelometer instrumentation.

The RH in the humidifier scans from low to high RH and back to low RH on an hourly basis. Figure A.2 below shows the hourly RH signals from the sensors in the system. RH and T sensors are located at the sample inlet to the impactor (sample); after a heater at the entrance to the reference nephelometer (heater); inside the reference nephelometer (ref); inside the humidified nephelometer (wet); and at the output of the humidified nephelometer (S2). The S2 sensor is the control sensor for the humidifier RH. In the *fRH* VAP, the RH inside the humidified nephelometer is calculated from the calculated dewpoint at the exit of nephelometer and the temperature inside the nephelometer. The internal nephelometer RH sensor is not used in calculations because of its slower response time and higher uncertainty.

The aerosol hygroscopic growth is a measure of the increase in aerosol scattering relative to a dry, “reference” scattering with changes in relative humidity. A common way to quantify this growth is the aerosol hygroscopic growth factor, *fRH*, which is the ratio of the aerosol scattering coefficient at 85% RH to that at 40% RH.

$$fRH = \sigma_{sp}(85\%) / \sigma_{sp}(40\%)$$

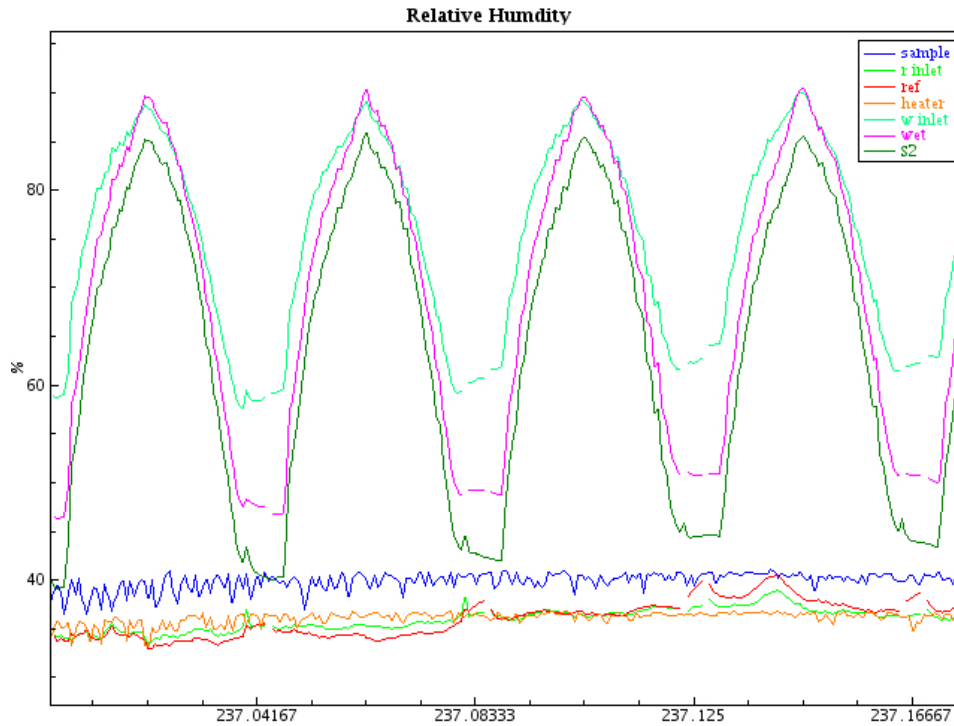


Figure A.2. Plot of relative humidity values versus day of year in 2010 for the AOS system at SGP.

The hygroscopic growth VAP is available in the ARM Data Archive as the xxxcmdlaosfithC1.c1 datastream, where xxx designates the site name (sgp, nsa, or one of the amf sites). The VAP model computes the fit parameters for the aerosol hygroscopic growth from both 2 and 3 parameter empirical fits of the data.

$$\sigma_{\text{sp}}(\text{wet})/\sigma_{\text{sp}}(\text{dry}) = a(1-\text{RH}_w/100)^{-\gamma} \quad (1)$$

$$\sigma_{\text{sp}}(\text{wet})/\sigma_{\text{sp}}(\text{dry}) = b(1+c(\text{RH}_w/100))^{-d} \quad (2)$$

The first 2-parameter fit is discussed by Hanel (1976) and the 3-parameter fit by Kotchenruther et al. (1999). Both models assume equilibrium (metastable) growth of the aerosol scattering with RH such that the humidigraph profile does not display a deliquescent growth profile. For aerosol in a humid environment, this behavior will hold true. Most aerosols are a mixture of metastable and deliquescent particles and will exhibit some deliquescent behavior. A quality check of the hygroscopic fit parameter data is the chi-square fit parameter, which indicates how well the data fit the calculated parameters. Another check of the appropriate use of such fits is the ambient RH or sample inlet RH. The likelihood of the aerosol displaying a deliquescent growth profile increases as the ambient RH declines. The metastable or deliquescent behavior of the aerosol will vary with composition. The “a” and “b” parameters in equations (1) and (2) will vary with aerosol loss in the humidifier, small differences in the instrument calibrations, and zeros. These parameters are not used typically in the calculation of the aerosol scattering at a specific RH. For calculation of the ambient state scattering, $\sigma_{\text{sp}}(\text{amb})$, from the 2-parameter fit, use the following equation.

$$\sigma_{sp}(amb) = \sigma_{sp}(dry) \frac{(1 - RH_{amb}/100)^{-\gamma}}{(1 - RH_{dry}/100)^{-\gamma}} \quad (3)$$

The figures below show humidigraph profiles and a 2-parameter fit of the data from 2010 at SGP.

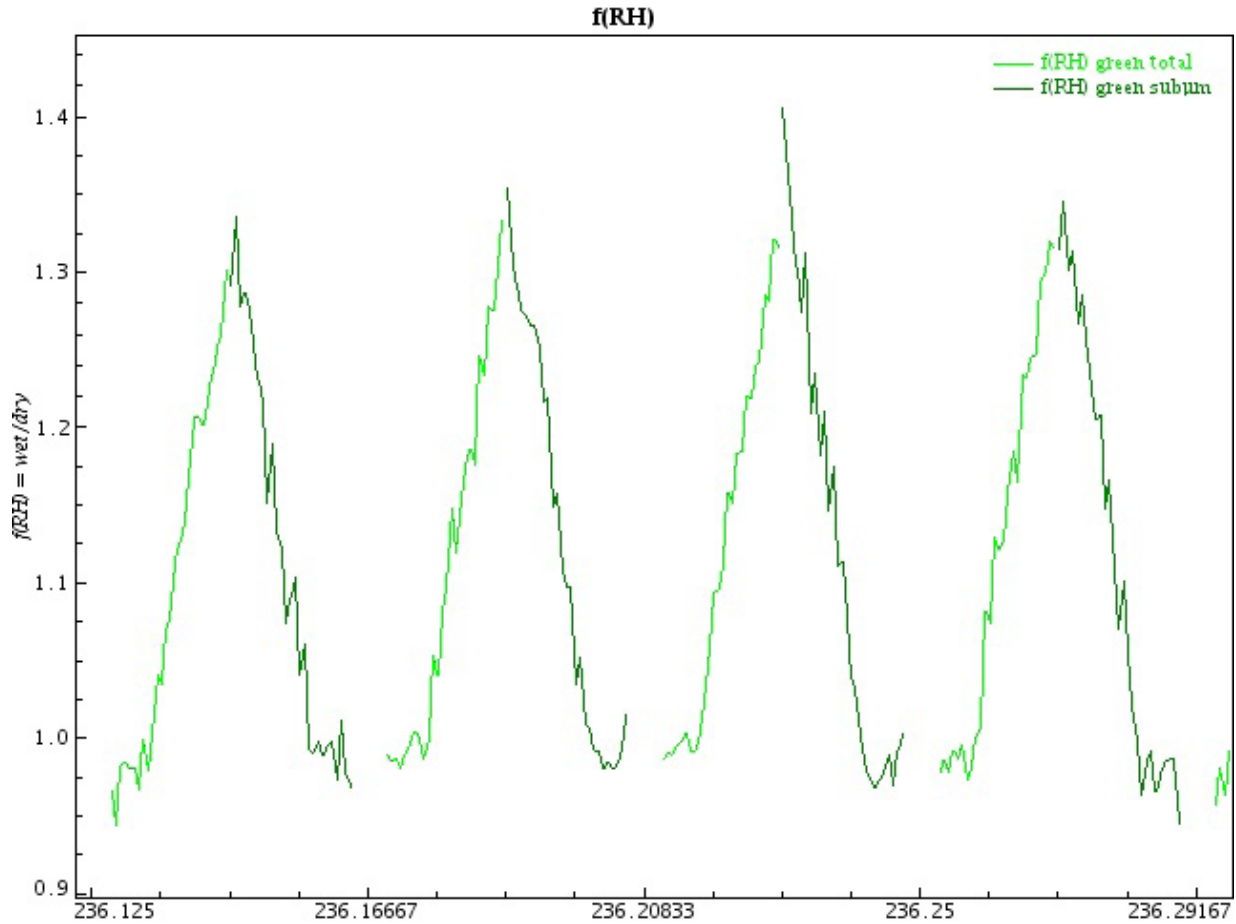


Figure A.3. Ratio of $\sigma_{sp}(\text{wet})/\sigma_{sp}(\text{dry})$ at 550 nm versus decimal day of year 2010. Four hours of data are shown. The first 30 minutes of each hour is sub-10-micron size aerosol (light green), and the last 30 minutes is submicron size aerosol (dark green).

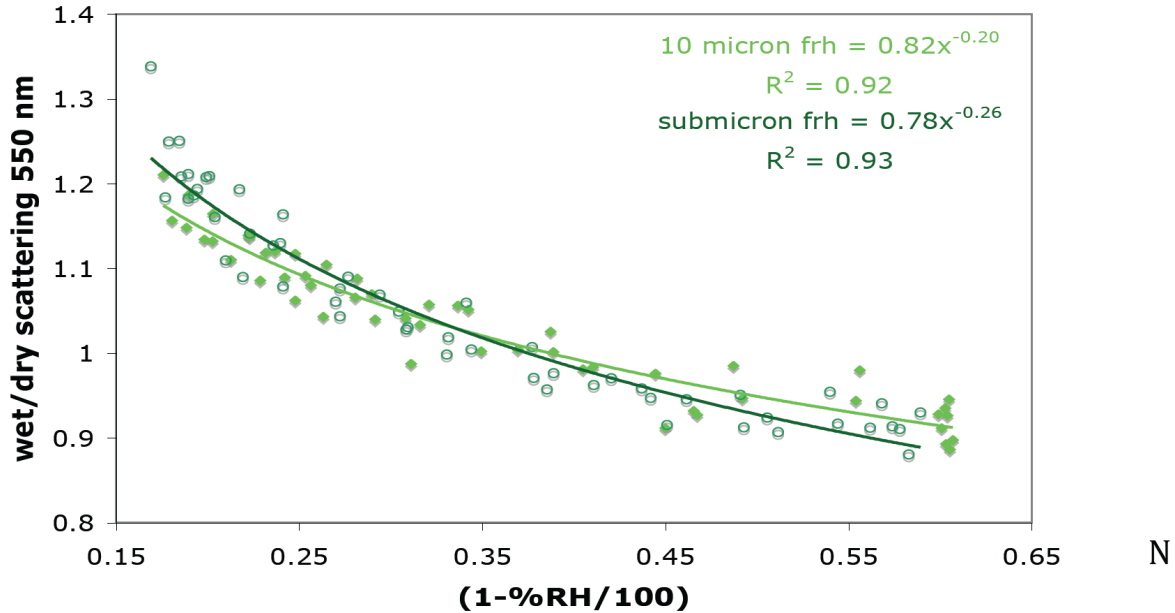


Figure A.4. Ratio of $\sigma_{sp}(\text{wet})/\sigma_{sp}(\text{dry})$ at 550 nm versus $(1-\%RH/100)$. The 2-parameter fit curves are for sub-10-micron (light green) and submicron (dark green) data from day 237 (August 25, 2010) at SGP. Two hours of data are shown with one-minute data integration.

References:

Hanel, G. 1976. "The properties of atmospheric aerosol particles as functions of the relative humidity at thermodynamic equilibrium with the surrounding moist air." *Advances in Geophysics* 19: 73–188.

Kotchenruther, RA, PV Hobbs, and DA Hegg. 1999. "Humidification factors of atmospheric aerosols off the mid-Atlantic coast of the United States." *Journal of Geophysical Research* 104: 2239–2251.

ARM xxxcmdlaosftrhC1.c1 netcdf file formats and operation dates

There are 4–5 parameters for each fit:

1. Calculated ratio of wet/dry scattering coefficients at 85/40 RH
2. fRH χ^2 Pearson's goodness of fit coefficient
- 3–5. fRH fit parameters.

There are 18 fits:

- Red, green, and blue wavelengths
- Sub-um, sub-10-um size aerosol
- Total and hemispheric back scattering coefficients
- 2 and 3 parameter fits
- Only the 2-parameter fits exist for the 6 backscattering values
- 2 and 3 parameter fits exist for the 6 total scattering values.

Fit boundary conditions:

All of the fits have between 14–27 one-minute data points. Humidigraph scans with less than 14 points have a missing value codes for their fit parameters.

The fits are truncated to start at a minimum RH of 40%. Below this %RH, the ratio of wet/dry scattering tends to be flat with changes in %RH. The fit quality decreases if data below 40% are included in the fit, as the fit assumes an increasing scattering ratio with RH.

The initial %RH of the humidigraph scan in the wet nephelometer has a maximum value of 65%. Fit parameters with initial %RH values above 65% in the wet nephelometer are replaced with missing value codes.

Fit parameters with fRH (85%/40%) fit parameters above 5.0 are replaced with missing value codes.

Operations dates of *f*RH measurements.

- SGP: January 1999–present
- NSA: September 2006–present
- PYE: July–September 2005
- NIM: December 2005–December 2006
- FKB: May–December 2007
- HFE: May–December 2008
- GRW: May 2009–December 2010
- PGH: May 2011–April 2012.

The netcdf file format is located on the ARM website at

<https://engineering.arm.gov/tool/dod/showdod.php?Inst=cmdlaosfitrh&View=dev>.

The basic format is given below. “X” refers to either a blue (B), green (G), or red (R) nephelometer wavelength, and * refers to either 10- or 1-um-size aerosol. The files give hourly fit values for either the sub-*um* or sub-10-*um* size aerosol. The one-minute data that went into the fits are located in the xxxaosC1.a1 data files, where xxx is the station identifier. All fits were performed using a Levenburg--Marquardt, nonlinear, least-squares fitting method.

File variables:

```
int base_time ;
double time_offset(time) ;
double time(time) ;
fRH_85by40_3param_*_Xum:long_name = "X wavelength, fitted value of f(RH) for 85/40, three
parameter fit, *um" ;
fRH_3param_chi_*_Xum:long_name = "X wavelength, goodness of fit parameter, three parameter fit,
*um" ;
```

fRH_Bs_X_*um_min:long_name = "X wavelength, minimum light scattering coefficient for wavelength reported by STP, *um" ;

fRH_RH_Dry_*um_min:long_name = "X wavelength, minimum dry relative humidity used in curve fit, *um" ;

fRH_RH_Dry_*um_max:long_name = "X wavelength, maximum dry relative humidity used in curve fit, *um" ;

fRH_RH_Wet_*um_min:long_name = "X wavelength, minimum wet relative humidity used in curve fit, *um" ;

fRH_RH_Wet_*um_max:long_name = "X wavelength, maximum wet relative humidity used in curve fit, *um" ;

fRH_3param_p1_X_*um:long_name = "X wavelength, three parameter curve fit, parameter 1, *um" ;

fRH_3param_p2_X_*um:long_name = "X wavelength, three parameter curve fit, parameter 2, *um" ;

fRH_3param_p3_X_*um:long_name = "X wavelength, three parameter curve fit, parameter 3, *um" ;

fRH_85by40_2param_X_*um:long_name = "X wavelength, fitted value of f(RH) for 85/40, two parameter fit, *um" ;

fRH_2param_chi_X_*um:long_name = "X wavelength, Goodness of fit parameter, two parameter fit, *um" ;

fRH_2param_p1_X_*um:long_name = "X wavelength, two parameter curve fit, parameter 1, 10um" ;

fRH_2param_p2_X_*um:long_name = "X wavelength, two parameter curve fit, parameter 2, *um" ;

fRH_85by40_Bbs_X_10um:long_name = "X wavelength, fitted value of f(RH) for 85/40 for bbsp, *um" ;

fRH_Bbs_X_*um:long_name = "X wavelength, fitted value of f(RH) for bbsp, *um";

fRH_Bbs_chi_X_*um:long_name = "X wavelength, goodness of fit, bbsp fit, *um" ;

fRH_Bbs_p1_X_*um:long_name = "X wavelength, parameter 1 for bbsp curve fit, *um"

fRH_Bbs_p2_X_*um:long_name = "X wavelength, parameter 2 for bbsp curve fit, *um"

Appendix B

Cloud Condensation Nuclei (CCN) Measurements

Cloud condensation nuclei (CCN) are particles that are capable of activating to form cloud droplets at a given percent super saturation (%ss). According to the Köhler equation, the vapor pressure or %ss above an aqueous drop will vary with the drop surface tension or size and the solute concentration or chemical composition. The AOS CCN measurements report the CCN concentration over a range of %ss values. The SGP site has complementary aerosol size, composition, and gRH measurements that can be used to predict CCN. CCN measurements are available from SGP, NSA, PYE, NIM, FKB, HFE, and GRW sites as well as future AMF2 and Darwin sites.

The CCN data are from ground-based and aircraft IOP in situ measurements. The surface sites measure the CCN concentration at several super saturations using a DMT single-column CCN counter (Roberts and Nenes 2005). The percent super saturation of the instrument is stepped through 7 intervals every 30 minutes with 5 minutes at each setting in a pyramid profile. The %ss in the CCN datastream is calculated using a heat transfer and fluid dynamics model flow model (Lance et al. 2006). The model uses the calibrated temperature, pressure, and flows in the instrument to calculate the %ss. Small variations in the %ss will arise from changes in the column thermal properties in the instrument. Rose et al. (2008) discusses the model and salt calibration calculations of the instrument %ss and uncertainty associated with thermal properties. The CCN instrument is serviced and calibrated at the beginning of each deployment for the mobile facility and annually for the SGP site. The CCN %ss stepping scheme and two hours of data appear in Figure B.1 below.

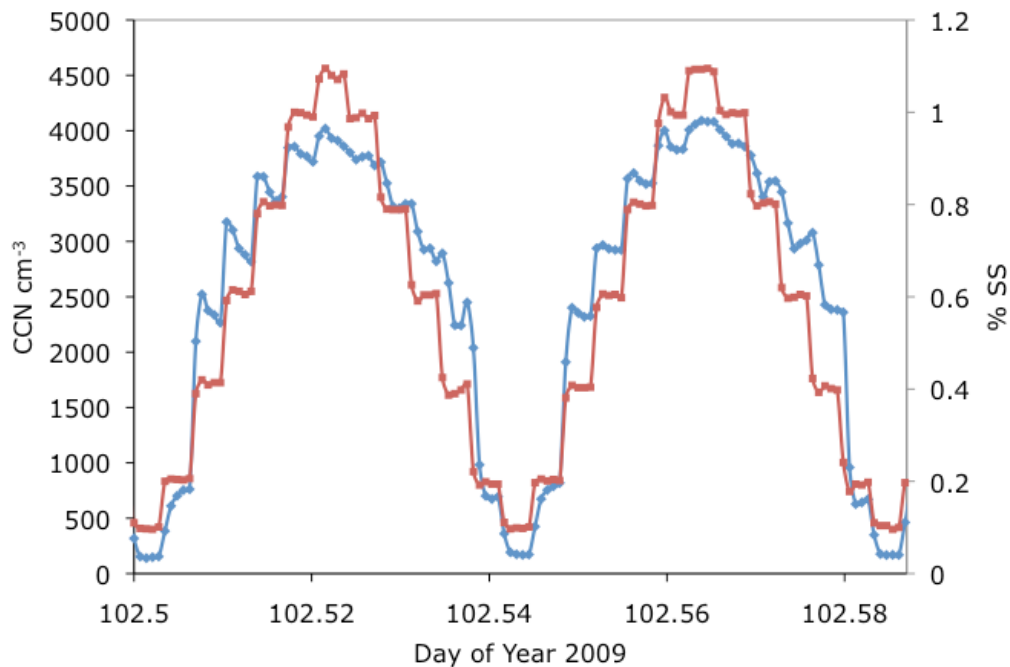


Figure B.1. Stepping scheme of %SS (red) and typical CCN number concentration (blue) on April 12, 2009, at SGP.

The first minute after a change in %ss, the CCN temperatures are not stable, and the %ss values usually overshoot the set point value. For this reason, the first minute of every %ss setting is disregarded, and only the last four minutes are averaged together. Rose et al. 2008 note a higher deviation of the %ss value from the calibration fit line at low %ss values. Care should be taken when using %ss values below 0.15, as the error in the calibrations is much higher than at higher %ss values. At very high particle concentrations, the instrument becomes water-limited, and a high fraction of the particles do not activate to droplets. Latham and Nenes (2011) present a correction scheme for the %ss decrease under conditions of high CN concentrations greater than 5000 cm⁻³.

The AOS CCN datastream `stnaosccnC1.a1.YYYYMMDD.*` contains the instrument raw data. “stn” refers to the station name, e.g. SGP. The data file has one-minute averaged data. The %ss value changes every 5 minutes. The differential temperature across the column and %ss value during the first minute of each %ss change is unstable and should not be used. There are two reported %ss values in the file: `CCN_ss_set(time)` is the %ss value reported by the instrument, and `CCN_ss_calc(time)` is the %ss value calculated from the Lance et al. 2006 model. The lowest size bin of the OPC detector is usually set to 1 micron. The instrument will count super-micron aerosol particles as CCN. This over-counting of CCN is a problem during times with unusually high number concentrations of large particles such as dust or sea salt. During known periods with high super micron particle concentrations, the lowest size bins can be eliminated from the total CCN number concentration, especially at the lowest %ss value. One-minute, mentor-edited CCN data is available in the `stnaosX1.a1.YYYYMMDD.*` datastream as the `N_CCN_1(time)` parameter.

The CCN raw data stream netcdf header file follows.

```
netcdf sgpaosccnC1.a1.20070612.000000 {
dimensions:
    time = UNLIMITED ; // (1440 currently)
    num_bins = 21 ;

variables:
    int base_time ;
        base_time:string = "11-Jun-2007,23:59:01 GMT" ;
        base_time:long_name = "Base time in Epoch" ;
        base_time:units = "seconds since 1970-1-1 0:00:00 0:00" ;
    double time_offset(time) ;
        time_offset:long_name = "Time offset from base_time" ;
        time_offset:units = "seconds since 2007-06-11 23:59:01 0:00" ;
    double time(time) ;
        time:long_name = "Time offset from midnight" ;
        time:units = "seconds since 2007-06-12 00:00:00 0:00" ;
    float CCN_ss_set(time) ;
        CCN_ss_set:long_name = "AOS CCN sample saturation setpoint value
        reported by instrument" ;
        CCN_ss_set:units = "%" ;
        CCN_ss_set:missing_value = -9999.f ;
    int CCN_temp_unstable_flag(time) ;
        CCN_temp_unstable_flag:long_name = "Hexadecimal flag, non-zero
```

```
value means instrument is not operating stably" ;
    CCN_temp_unstable_flag:units = "unitless" ;
    CCN_temp_unstable_flag:missing_value = -9999 ;
    CCN_temp_unstable_flag:bit_1 = "(0x02) set by CPD, based on standard
    deviation of column temperature difference (threshold exceeded)" ;
float CCN_T_TEC1(time) ;
    CCN_T_TEC1:long_name = "AOS CCN temperature at top of column" ;
    CCN_T_TEC1:units = "degrees C" ;
    CCN_T_TEC1:missing_value = -9999.f ;
float CCN_T_TEC2(time) ;
    CCN_T_TEC2:long_name = "AOS CCN temperature at middle of
    column" ;
    CCN_T_TEC2:units = "degrees C" ;
    CCN_T_TEC2:missing_value = -9999.f ;
float CCN_T_TEC3(time) ;
    CCN_T_TEC3:long_name = "AOS CCN temperature at bottom of
    column" ;
    CCN_T_TEC3:units = "degrees C" ;
    CCN_T_TEC3:missing_value = -9999.f ;
float CCN_T_sample(time) ;
    CCN_T_sample:long_name = "AOS CCN temperature of sample air
    entering the column" ;
    CCN_T_sample:units = "degrees C" ;
    CCN_T_sample:missing_value = -9999.f ;
float CCN_T_inlet(time) ;
    CCN_T_inlet:long_name = "AOS CCN temperature of sample air at
    entrance to instrument" ;
    CCN_T_inlet:units = "degrees C" ;
    CCN_T_inlet:missing_value = -9999.f ;
float CCN_T_OPC(time) ;
    CCN_T_OPC:long_name = "AOS CCN temperature of the optical particle
    counter" ;
    CCN_T_OPC:units = "degrees C" ;
    CCN_T_OPC:missing_value = -9999.f ;
float CCN_T_nafion(time) ;
    CCN_T_nafion:long_name = "AOS CCN temperature of the nafion
    humidifier" ;
    CCN_T_nafion:units = "degrees C" ;
    CCN_T_nafion:missing_value = -9999.f ;
float CCN_dT_TEC3_TEC1_StdDev(time) ;
    CCN_dT_TEC3_TEC1_StdDev:long_name = "AOS CCN standard
    deviation of difference (CCN_T_TEC1 - CCN_T_TEC3)" ;
    CCN_dT_TEC3_TEC1_StdDev:units = "degrees C" ;
    26
    CCN_dT_TEC3_TEC1_StdDev:missing_value = -9999.f ;
```

```

float CCN_Q_sample(time) ;
    CCN_Q_sample:long_name = "AOS CCN volumetric flowrate of sample
    air" ;
    CCN_Q_sample:units = "cm^3/minute" ;
    CCN_Q_sample:missing_value = -9999.f ;
float CCN_Q_sheath(time) ;
    CCN_Q_sheath:long_name = "AOS CCN volumetric flowrate of sheath
    air" ;
    CCN_Q_sheath:units = "cm^3/minute" ;
    CCN_Q_sheath:missing_value = -9999.f ;
float CCN_P_sample(time) ;
    CCN_P_sample:long_name = "AOS CCN sample pressure" ;
    CCN_P_sample:units = "hPa" ;
    CCN_P_sample:missing_value = -9999.f ;
float CCN_laser_current(time) ;
    CCN_laser_current:long_name = "AOS CCN OPC laser current" ;
    CCN_laser_current:units = "mA" ;
    CCN_laser_current:missing_value = -9999.f ;
float N_CCN(time) ;
    N_CCN:long_name = "AOS number concentration of CCN" ;
    N_CCN:units = "1/cm^3" ;
    N_CCN:missing_value = -9999.f ;
    int N_CCN_bin_number(time) ;
    N_CCN_bin_number:long_name = "AOS bin number of lowest channel
    of OPC include in summation of N_CCN" ;
    N_CCN_bin_number:units = "unitless" ;
    N_CCN_bin_number:missing_value = -9999 ;
float N_CCN_dN(time, num_bins) ;
    N_CCN_dN:long_name = "AOS CCN number concentration by bin " ;
    N_CCN_dN:units = "unitless" ;
    N_CCN_dN:missing_value = -9999.f ;
    N_CCN_dN:comment1 = "Each bin contains a droplet count, based on
    droplet size" ;
    N_CCN_dN:comment2 = "Bin droplet size (top of each bin) are
    0.75um, 1.0um, 1.5um, 2.0um, 2.5um ... to 10um in 0.5um increments" ;
float CCN_ss_calc(time) ;
    CCN_ss_calc:long_name = "AOS CCN sample supersaturation
    calculated by model" ;
    CCN_ss_calc:units = "%" ;
    CCN_ss_calc:missing_value = -9999.f ;
    CCN_ss_calc:model_documentation1 = "Roberts, G. C. and Nenes, A.
    (2005)" ;
    CCN_ss_calc:model_documentation2 = "A continuous-flow streamwise
    thermal-gradient CCN chamber for atmospheric measurements." ;
    CCN_ss_calc:model_documentation3 = "Aerosol Sci. Tech., 39, 206-
    221" ;

```

27

```
CCN_ss_calc:model_documentation4 = "Lance, S., Medina, J., Smith, J. N.
and Nenes, A. (2006)";
CCN_ss_calc:model_documentation5 = "Mapping the operation of
the DMT continuous flow CCN counter";
CCN_ss_calc:model_documentation6 = "Aerosol Sci. Tech., 2006";
float CCN_UpperSizeLimit(num_bins);
  CCN_UpperSizeLimit:long_name = "Size of upper limit of each CCN bin";
  CCN_UpperSizeLimit:units = "um";
  CCN_UpperSizeLimit:missing_value = -9999.f;
float CCN_FirstStageMonitorVoltage(time);
  CCN_FirstStageMonitorVoltage:long_name = "First stage monitor
voltage";
  CCN_FirstStageMonitorVoltage:units = "V (DC)";
  CCN_FirstStageMonitorVoltage:missing_value = -9999.f;
float CCN_Temperature_Gradient(time);
  CCN_Temperature_Gradient:long_name = "CCN temperature gradient";
  CCN_Temperature_Gradient:units = "C";
  CCN_Temperature_Gradient:missing_value = -9999.f;
float CCN_ProportionalValveVoltage(time);
  CCN_ProportionalValveVoltage:long_name = "CCN Propotional
valve voltage";
  CCN_ProportionalValveVoltage:units = "V";
  CCN_ProportionalValveVoltage:missing_value = -9999.f;
float lat;
  lat:long_name = "north latitude";
  lat:units = "degrees";
  lat:valid_min = -90.f;
  lat:valid_max = 90.f;
float lon;
  lon:long_name = "east longitude";
  lon:units = "degrees";
  lon:valid_min = -180.f;
  lon:valid_max = 180.f;
float alt;
  0alt:long_name = "altitude";
```

References:

Lance, S, J Medina, JN Smith, and A Nenes. 2006. "Mapping the operation of the DMT continuous flow CCN counter." *Aerosol Science and Technology* 40(4): 242–254.

Lathem, TL, and A Nenes. 2011. "Water vapor depletion in the DMT continuous flow CCN chamber: effects on supersaturation and droplet growth." *Aerosol Science and Technology*, in press.

Roberts, G, and A Nenes. 2005. "A continuous-flow streamwise thermal- gradient CCN chamber for atmospheric measurements." *Aerosol Science and Technology* 39(3): 206–221.

Rose, D, SS Gunthe, E Mikhailov, GP Frank, U Dusek, MO Andreae, and U Poschl. 2008. "Calibration and measurement uncertainties of a continuous-flow cloud condensation nuclei counter (DMT-CCNC): CCN activation of ammonium sulfate and sodium chloride aerosol particles in theory and experiment." *Atmospheric Chemistry and Physics* 8: 1153–1179.



U.S. DEPARTMENT OF
ENERGY

Office of Science